EV PD-L1 Contributes to Immunosuppressive CD8+ T Cells in Peripheral Blood of Pediatric Wilms Tumor

Xiaoxue Zhang, MD[1], Zongran Liu, PhD[2], Yiran Hou, SH[3],
Hong Jiao, AST[4], Junli Ren, MD[5], and Guoliang Wang, PhD[4] (iD)

Abstract

Wilms tumor (WT) is the most common renal cancer and the most prevalent abdominal cancer in children. Children with recurrent or progressive forms of WT could benefit from novel immune-targeted approaches. While the immune status of these patients, especially the immunosuppression of peripheral T cells, was rarely reported. The present study enrolled a consecutive series of 14 Chinese WT children and 14 age- and gender-matched healthy controls. We demonstrated that plasma extracellular vesicular (EV) PD-L1 levels significantly increased in WT patients than in healthy controls. EV PD-L1 significantly inhibited the activation of human CD8+ T cells by down-regulating the cell surface CD69 expression and the intracellular IFNγ and TNFα production in vitro. In peripheral CD8+ T cells of WT patients, the intracellular IFNγ and TNFα production significantly decreased than healthy controls. The level of plasma EV PD-L1 significantly correlated with the intracellular TNFα production in peripheral CD8+ T cells of WT patients. In conclusion, the significantly increased plasma EV PD-L1 in WT patients contributed to the immunosuppression of peripheral CD8+ T cells. Monitoring the level of plasma EV PD-L1 will be helpful for the selection of immune-targeted therapies for WT patients.

Introduction

Wilms tumor (WT), also known as nephroblastoma, is the most common renal cancer and the most prevalent abdominal cancer in children.[1,2] Although 90% of WT being demonstrated as "favorable" histology and respond well to effective treatments, recurrence occurs in about 15% of WT children with favorable pathological types. And the survival rates of unfavorable histology ranges from 84% to 38%, depending on the disease stage.[2-4] Children with recurrent or progressive forms of WT could benefit from novel immune-targeted approaches.

In recent years, immune checkpoint protein inhibitors, especially antibodies against programmed death-ligand 1 (PD-L1) and programmed death-1 (PD-1), have proven to be a

[1] Xiang'an Hospital of Xiamen University, Xiamen, Fujian, China
[2] Department of Pathology, Peking University Health Science Center, Beijing, China
[3] The Affiliated High school of Peking University, Beijing, China
[4] National Center for Children's Health (NCCH), Beijing Pediatric Research Institute, Beijing Children's Hospital, Capital Medical University, Beijing, China
[5] Shanxi Provincial Cancer Hospital, Taiyuan, Shanxi, China

Corresponding Authors:
Guoliang Wang, National Center for Children's Health (NCCH), Beijing Pediatric Research Institute, Beijing Children's Hospital, Capital Medical University, No. 56 Nanlishi Road, Beijing, China.
Email: wgl163@126.com

Junli Ren, Department of Radiotherapy Abdominophenaceae, Shanxi Provincial Cancer Hospital, No. 3 Zhigong Xincun, Xinghualing District, Taiyuan, Shanxi, China.
Email: renjunli8499@163.com

revolutionary therapy against many types of tumors.[5-7] As a membrane-bound ligand, PD-L1 has been reported upregulated in almost all types of tumors and associated with poor prognosis.[8] Tumor PD-L1 could suppress the cell proliferation, cytokine secretion, and cytotoxicity of infiltrated CD8^{+} T cells, through binding to the PD-1 receptor.[9,10] Therapeutic antibodies, by blocking the interaction between PD-L1 and PD-1, can reactivate the anti-tumor T-cell response.[11,12] However, recent studies demonstrated that PD-L1 can also be expressed on the surface of extracellular vesicles (EV) and EV PD-L1 (ePD-L1) levels have been associated with tumor progression in some types of adult cancer.[13-16] Tumor-derived EVs also reported can regulate the tumor-infiltrating lymphocytes[17] and exosomes isolated from plasma of cancer patients demonstrated immunosuppressive activity.[18,19] For the low response rate of anti-PD-L1/PD-1 therapy on cancer patients,[20-22] the presence of PD-L1 on plasma EVs may be one of the important reasons. The association of EV PD-L1 with pediatric tumors is rarely reported. And there is no report about the association of EV PD-L1 with the function of peripheral T cells in pediatric tumors.

The present study aims to demonstrate whether the plasma concentration of ePD-L1 was increased in WT children and the role of ePD-L1 on CD8^{+} T-cell activation. The function of peripheral CD8^{+} T cells in WT children was also compared with that of healthy controls. These results are helpful to reveal the mechanisms by which tumor cells systemically suppress the immune system in pediatric tumors, especially in WT.

Materials and Methods

Patients and Sampling

A consecutive series of 14 Chinese WT children who were first treated at Beijing Children's Hospital between the years 2018 and 2019 were recruited to the study (Table 1). At the same time, 14 age- ($U = 70$, $P = .2050$) and gender-matched ($U = 91$, $P > .9999$) healthy Chinese children were also enrolled in this study as controls. Peripheral blood specimens (2–4 mL) were collected before treatment and centrifuged at 1000g for 10 min at room temperature. Plasma samples were collected and centrifuged again for 15 min 2500g at room temperature to obtain platelet-free plasma, which was stored in aliquots at −70 °C. This study was approved by Beijing Children's Hospital Ethics Committee (2017-53). All human subjects or their parents had provided written informed consent.

Isolation of EVs

EVs were isolated using the Total Exosome Isolation Kit (from plasma) (ThermoFisher Scientific) according to the manufacturer's instructions. Briefly, frozen platelet-free plasma was thawed immediately before EV isolation and diluted 1:1 in PBS. The diluted plasma samples were added 0.2 volume of Exosome Precipitation Reagent (from plasma). The resulting mixture was incubated at room temperature for 10 min and then centrifuged at 10 000g for 5 min at 4 °C. The supernatant was carefully aspirated and the pellet was resuspended into 50 µL of PBS.

Characterization of EVs

Morphological examination of isolated EVs was done using a transmission electron microscope. Forty microlitres of isolated EVs were fixed with 4% paraformaldehyde and were loaded on a 300-mesh copper grid. After stained with 2% phosphotungstic acid for 1 to 2 min, the EV samples were dried using an electric incandescent lamp for 10 min. Data were acquired using a transmission electron microscope (JEOL JEM-2100) at an accelerating voltage of 160 kV.

The number and size of EVs were examined using a NanoSight NS300 with a 405 nm laser instrument (Malvern Instruments, United Kingdom), as our previously described.[23] The camera level was maintained at 10 for light scatter mode. Three videos of typically 60 s duration were taken, with a frame rate of 30 frames per second. For optimal results, microvesicle concentrations were adjusted to obtain ~50 microvesicles per field of view. Data were analyzed by NTA 3.0 software (Malvern Instruments).

Immunostaining and Imaging of Plasma EVs

Platelet-free plasma samples were centrifuged first at 2500g for 10 min at room temperature, then FITC-anti-CD63 (10 µg/mL) and PerCP-anti-PD-L1(10 µg/mL) were added into the plasma samples for 2 h at room temperature. Then the plasma EVs were purified using Total Exosome Isolation Kit (from plasma) and resuspended with 20 µL PBS. The fluorescent-stained EVs were then smeared on a glass slide and visualized using a laser-scanning confocal microscope (TCS SP8 STED, Leica, magnification 63×10). The percentage of

Table 1. The clinical information of patients with Wilms tumor.

Patient's code	Gender	Age (year)	Disease stage	EV PD-L1 (pg/mL)
1	Female	1.5	2	40.63
2	Male	2.6	1	12.98
3	Female	4.1	3	32.05
4	Female	0.4	1	10.00
5	Male	2.7	2	10.14
6	Male	6.7	1	11.96
7	Male	2.2	1	18.34
8	Female	6.3	5	51.76
9	Female	2.1	2	28.91
10	Male	3.3	4	64.78
11	Female	0.9	1	10.00
12	Male	2.0	3	22.42
13	Female	0.8	1	27.76
14	Female	1.0	3	15.31

Disease stage was defined according to National Wilms' Tumor Study (NWTS).[2] Plasma EV PD-L1 concentration of WT patients was performed through ELISA.
Abbreviation: EV PD-L1, extracellular vesicular programmed death-ligand 1.

PD-L1-positive EVs from 5 randomly selected high power fields (magnification $4 \times 63 \times 10$) was calculated.

ELISA Assay

For detection of PD-L1 on EVs, Human B7H1/PD-L1 ELISA Kit was used according to the manufacturer's instructions (RayBioetch). The EVs derived from the plasma of patients and controls were prepared using the same volume of PBS as the plasma they were originally derived from. For samples lower than the minimum detectable concentration of PD-L1, a re-examination was performed using a quantity four times of the standard dose. Then, the minimum detectable PD-L1 concentration was 10 pg/mL in this study.

Figure 1. Significantly increased plasma EV PD-L1 of WT patients. Plasma EVs were isolated using the Total Exosome Isolation Kit. Representative transmission electron microscope image of EV (a) and representative NTA results of a 20-fold diluted EV solution (b) were shown. (c) Plasma EV PD-L1 (ePD-L1) concentration of WT patients and healthy controls was performed through ELISA and shown as a scatter plot. Comparison between groups was performed using a non-parametric Mann–Whitney U-test. (d) The Spearman correlation between plasma ePD-L1 concentration and patients' stage was shown.
Abbreviations: EV, extracellular vesicular; ePD-L1, extracellular vesicles PD-L1; WT, Wilms tumor.

T-Cell Suppression by EVs From WT Patients

Peripheral blood mononuclear cells (PBMCs) were isolated from fresh whole blood of healthy donors using Ficoll gradient. T cells (4×10^5/well) were cultured with RPMI 1640 medium (Gibco) in 48-well plates and activated with anti-CD3/anti-CD28 antibody-coated beads (4%, StemCell Technologies) and IL2 (150 IU/mL) for 6 h at 37 °C. The activated T cells were treated with EVs (with high PD-L1 content from WT patients and low PD-L1 content from controls) or PBS (as negative controls) for 24 h at 37 °C. T cells were then harvested and cell surface marker and intracellular cytokine staining for flow cytometry analysis were performed (see below).

T-Cell Phenotype and Intracellular Cytokine Staining Analysis by Flow Cytometry

T-cell surface marker staining and intracellular cytokine staining for flow cytometry analysis were performed as described previously.[23,24] In brief, freshly isolated PBMCs (Ficoll-Hypaque density gradients centrifugation) from fresh whole blood were stimulated with Phorbol-12-myristate-13-acetate (PMA, 50 ng/mL; Sigma-Aldrich) and ionomycin (1 µg/mL; Sangon Biotech) for 4 h. Cell surface staining was performed for 30 min at room temperature followed by fixation and permeabilization using an intracellular staining assay (BD Biosciences) according to the manufacturer's instructions. Cells were then stained with PE-anti-TNFα (Mouse IgG1, clone MAb11), APC-anti-IFNγ (Mouse IgG1, clone B27), or corresponding isotype control antibodies (all from BD Biosciences) at 4 °C for 30 min. Samples were then washed with PBS and data were acquired using FACSymphony flow cytometry. At least 20 000 CD3$^+$ lymphocytes were collected for each sample. Data analysis was performed using FlowJo software (Tree Star). The antibodies used for surface staining included APC-Cy7-anti-CD3 (clone HIT3a), PerCP-Cy5.5-anti-PD-1 (clone EH12.2H7), APC-anti-CD4 (clone OKT4), all from BioLegend, and FITC-anti-CD8 (clone RPA-T8), PE-Cy7-anti-CD8 (clone RPA-T8), PE-anti-CD28 (clone CD28.2), APC-anti-CD69 (clone FN50), all from BD Biosciences.

Statistical Analysis

Data are presented as the median ($Q1$, $Q3$). Non-parametric Mann–Whitney U-test was used for comparison between the groups. Correlations between two continuous variables were determined by Pearson's coefficient. The correlation between ePD-L1 and patients' stage was determined by non-parametric Spearman correlation. A bilateral P-value of <.05 was regarded as significant. Statistical analyses and graphing were performed using GraphPad Prism 8.

Results

Significantly Increased ePD-L1 Levels in Plasma of WT Patients

Plasma EVs were isolated using the Total Exosome Isolation Kit and identified by transmission electron microscopy
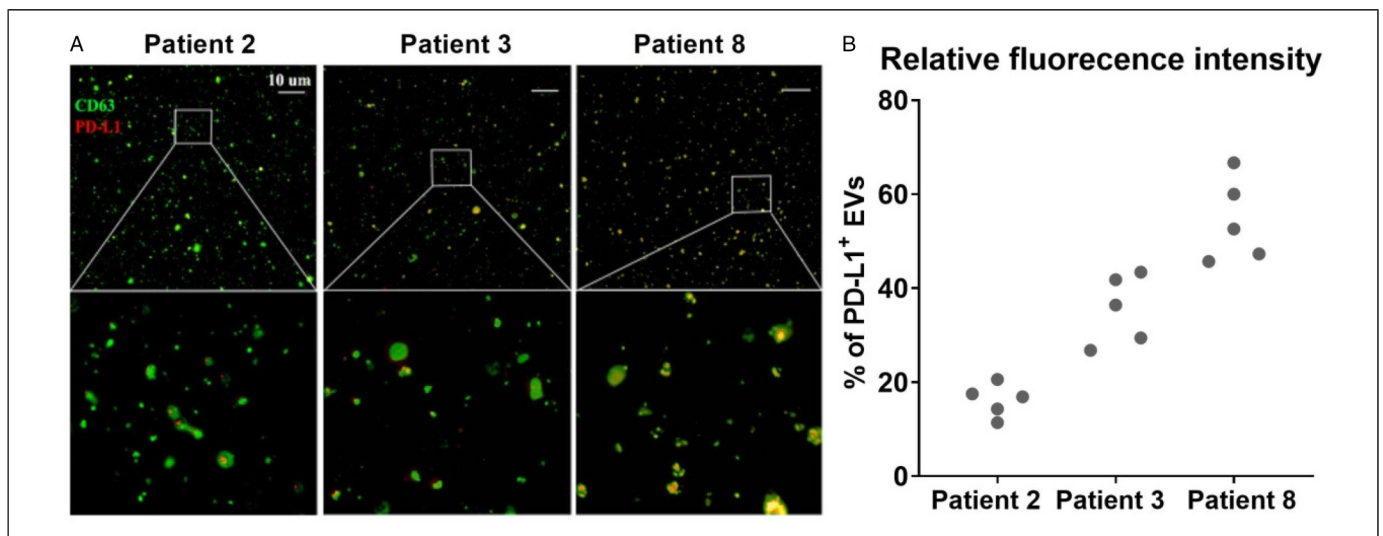

Figure 2. Immunostaining and confocal microscopy images of plasma ePD-L1 of 3 WT patients. A platelet-free plasma of 3 WT patients (with low, intermediated, and high ePD-L1 expression, respectively, as shown in Table 1) were stained with FITC-anti-CD63 (10 µg/mL) and PerCP-anti-PD-L1(10 µg/mL) for 2 h at room temperature, then plasma EVs were purified and resuspended with 20 µL PBS. The fluorescent-stained EVs were then smeared on a glass slide and visualized using a laser-scanning confocal microscope (TCS SP8 STED, Leica). The percentage of PD-L1-positive EVs from five randomly selected high power fields (magnification $4 \times 63 \times 10$) was calculated. The representative confocal microscope image (a) and quantification of PD-L1-positive EVs of these three WT patients (b) were shown.
Abbreviations: ePD-L1, extracellular vesicles PD-L1; EV, extracellular vesicles; WT, Wilms tumor.
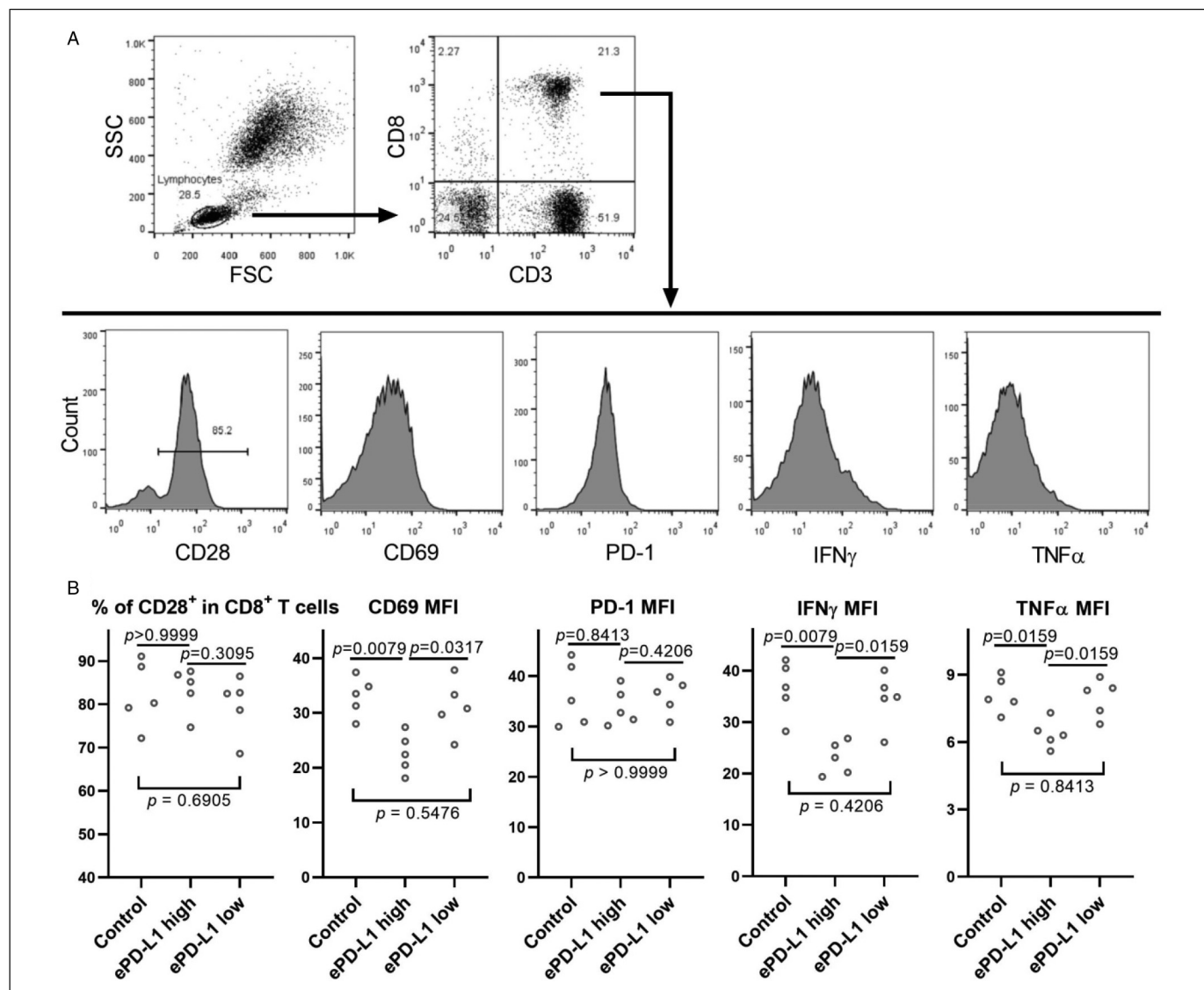
Figure 3. ePD-L1 inhibits the activation of human CD8+ T cells in vitro. Human PBMCs from healthy donors were isolated and cultured in a 48-well plate. The PBMCs were activated with anti-CD3/anti-CD28 antibody and were treated with EVs with high (>20 pg/mL; from WT patients) or low (<10 pg/mL; from healthy donors) PD-L1 expression, or treated with PBS as control. Cell surface marker and intracellular cytokine staining for flow cytometry analysis were performed. Representative histograms of flow cytometry analysis were shown (a). (b) The percentage of CD28+, and the MFI of CD69, PD-1, IFNγ, and TNFα in CD8+ T cells of the group of control, ePD-L1 high and ePD-L1 low were shown as scatter plots. Statistical analysis was performed using a non-parametric Mann–Whitney U-test.

Abbreviations: ePD-L1, extracellular vesicles PD-L1; MFI, mean fluorescent intensity; PBMCs, peripheral blood mononuclear cells.

(Figure 1a) and nanoparticle tracking analysis (NTA) (Figure 1b). The exosomes (smaller than 200 nm in diameter) account for about 95.5% of plasma EVs according to the results of NTA. The WT children exhibited significantly higher plasma ePD-L1 concentration compared with that of controls ($U = 51$, $P = .0284$), as shown in Figure 1c. The plasma ePD-L1 concentration of WT patients significantly correlated with WT stage ($r = 0.6913$, $P = .0083$), as shown in Figure 1d.

The differential expression of PD-L1 in peripheral EVs of WT children was further confirmed with confocal microscopy imaging by randomly selected 3 WT patients with

low, intermediate, and high plasma ePD-L1 concentration. The percentage of PD-L1-positive EVs from five randomly selected high power fields was calculated, as shown in Figure 2.

ePD-L1 Contributes to Immunosuppression of CD8+ T Cells In Vitro

The role of ePD-L1 on CD8+ T-cell function was assessed. The isolated normal human T cells were activated and co-incubated with PD-L1high (from WT children) or PD-L1low (from healthy

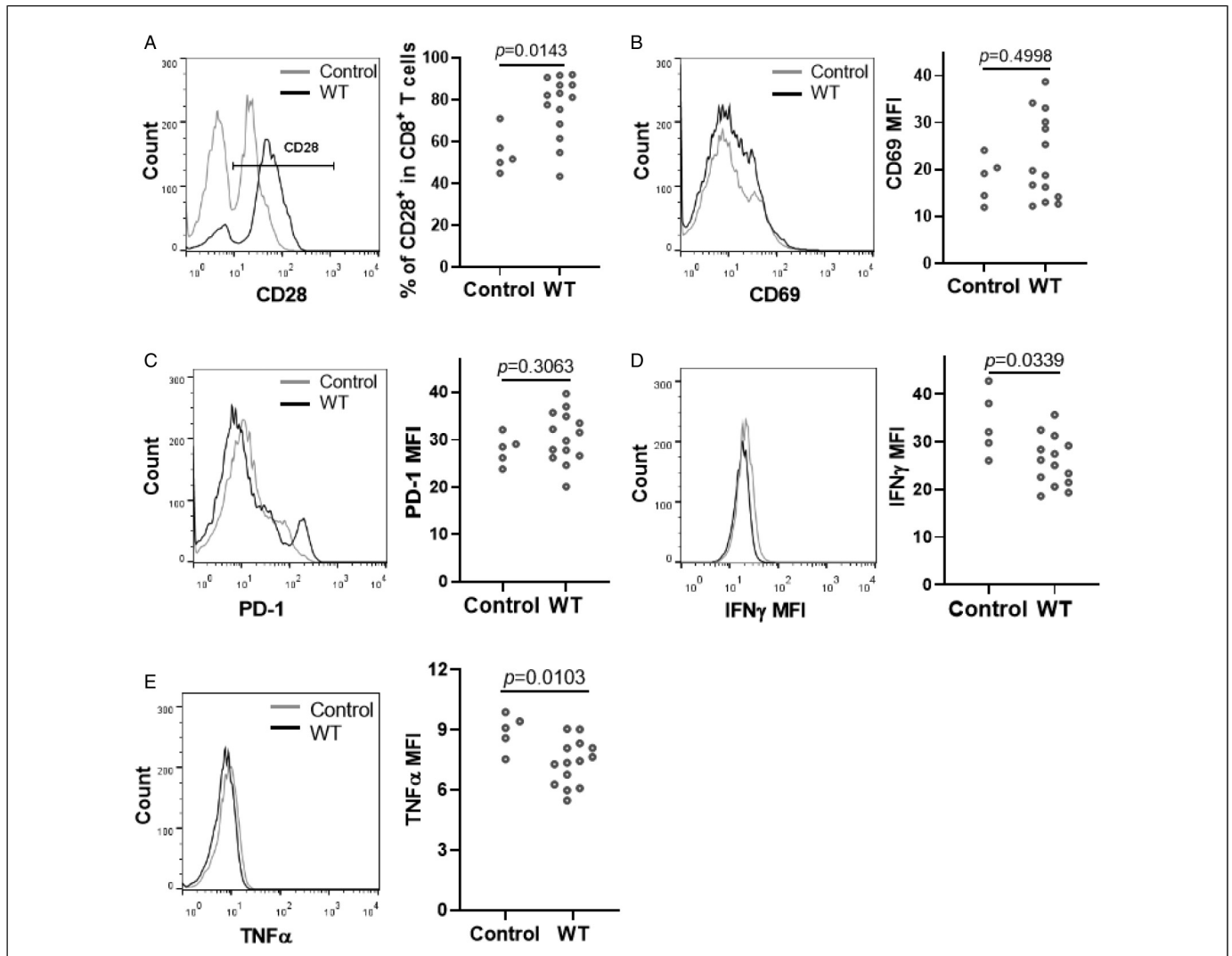**Figure 4.** Inhibited peripheral CD8$^+$ T cells of WT patients. PBMCs from WT patients or healthy controls (plasma ePD-L1 <10 pg/mL) were isolated and stimulated with Phorbol-12-myristate-13-acetate and ionomycin for 4 h. Cell surface markers (CD28, CD69, and PD-1) and intracellular IFNγ and TNFα staining for flow cytometry analysis were performed. Representative histograms of flow cytometry analysis were shown. The percentage of CD28$^+$, and the MFI of CD69, PD-1, IFNγ, and TNFα in CD8$^+$ T cells of WT patients and controls were shown as scatter plots (a–e). Statistical analysis was performed using a non-parametric Mann–Whitney *U*-test.
Abbreviations: ePD-L1, extracellular vesicles PD-L1; MFI, mean fluorescent intensity; PBMCs, peripheral blood mononuclear cells; WT, Wilms tumor.

controls) EVs in vitro. The activated human CD8$^+$ T cells demonstrated upregulated surface CD28, CD69, and PD-1 expression as well as increased intracellular IFNγ and TNFα production. Following co-culture of these T cells with PD-L1^{high} EVs, levels of CD69, IFNγ, and TNFα decreased significantly (Figure 3b). The expression levels of surface CD28 and PD-1 in CD8$^+$ T cells had not decreased significantly under the treatment of PD-L1^{high} EVs (Figure 3b). Contrary to the PD-L1^{high} EVs, co-culture of T cells with PD-L1^{low} EVs did not significantly decrease the levels of CD69, IFNγ, or TNFα (Figure 3b). These results demonstrated that the EVs (with high PD-L1 level) of WT children are biologically active in interfering with the activation of effecter CD8$^+$ T cells.

Plasma ePD-L1 Levels Correlated with Inhibited Peripheral CD8$^+$ T-Cell Function of WT Patients

The peripheral CD8$^+$ T-cell function of WT patients was investigated by flow cytometry. Compared with peripheral CD8$^+$ T cells from healthy control, peripheral CD8$^+$ T cells from WT patients had significantly increased proportion of CD28$^+$ cells ($U = 9$, $P = .0143$, Figure 4a), and significantly decreased intracellular IFNγ ($U = 12$, $P = .0339$, Figure 4d) and TNFα ($U = 8$, $P = .0103$, Figure 4e) levels. The correlations of significantly changed markers (CD28, IFNγ and TNFα) with plasma ePD-L1 levels were then assessed, as is shown in Figure 5. The plasma ePD-L1 levels significantly negatively correlated with the intracellular TNFα production ($r = -0.6001$, $P =$
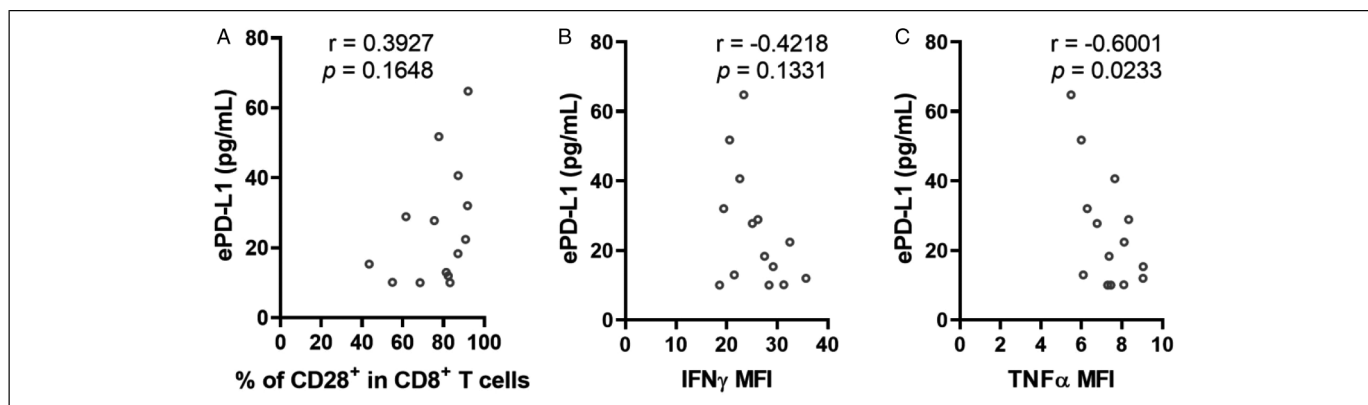
Figure 5. Correlation of plasma ePD-L1 with markers of peripheral CD8^{+} T cells in WT patients. The Pearson coefficients of the plasma ePD-L1 concentrations with expression levels of significantly changed markers (CD28, IFNγ, and TNFα, as shown in Figure 4) in peripheral CD8^{+} T cells of WT patients were calculated.
Abbreviations: ePD-L1, extracellular vesicles PD-L1; WT, Wilms tumor.

.0233, Figure 3f) of peripheral CD8^{+} T cells. While the plasma ePD-L1 levels were not correlated with the cell surface CD28 expression ($r = 0.3927$, $P = .1648$, Figure 5a) or intracellular IFNγ production ($r = -0.4218$, $P = .1331$, Figure 5b).

Discussion

Although improved therapies have greatly increased the survival rate of WT, recurrence occurs in about half of WT children.[25] The survival rate of unfavorable histology ranges from 84% to 38%.[2-4] On the other hand, immune checkpoint inhibitors, especially antibodies against PD-L1/PD-1, have made great progress in cancer treatment in recent years. It is feasible to treat recurrent or unfavorable-histological WT with immune checkpoint inhibitors. Recent studies reported the association of plasma ePD-L1 with the low response rate of anti-PD-L1/PD-1 therapy on cancer patients.[20-22] It is interesting to study the expression level of plasma ePD-L1 in WT patients and to explore its role on T cells.

The present study demonstrated that the plasma concentration of ePD-L1 was significantly increased in WT children compared with that in healthy controls. Through immunofluorescent staining and confocal microscopy imaging, we confirmed the expression of PD-L1 on EVs. The results of NTA indicated that more than 95% of plasma extracellular vesicles were exosomes (30–200 nm in diameter). This demonstrated that exosome PD-L1 accounts for the vast majority of plasma extracellular membrane-bounded PD-L1 in WT children.

It has been reported that tumor cell-derived exosomes contributed to immunosuppression through membrane PD-L1.[13,14] By investigating the role of EVs, from WT patients (with higher PD-L1 expression) and from healthy controls (with lower PD-L1 expression), on the activation of cultured human CD8^{+}T cells, we demonstrated that EVs form WT patients significantly decreased the expression of cell surface CD69, intracellular IFNγ and intracellular TNFα production. These results indicated that increased ePD-L1 concentrations in WT patients

were involved in the inhibition of CD8^{+} T-cell activation. Our results are consistent with previous findings that EVs or exosomes from cancer patients mediate the immune suppression of activated T cells.[13-16,23]

In order to explore the immune-suppression status of peripheral CD8^{+} T cells in WT patients, we compared the function of peripheral CD8^{+} T cells in WT children and healthy controls. Results show that the peripheral CD8^{+} T cells of WT patients had significantly decreased intracellular IFNγ and TNFα production, although the expression level of CD28 was increased in peripheral CD8^{+} T cells of WT patients. These results demonstrated the in situ immunosuppression of plasma ePD-L1 against peripheral CD8^{+} T cells in WT. Our results are consistent with Poggio's report that suppression of ePD-L1 could induce systemic anti-tumor immunity.[26] In this context, the plasma level of ePD-L1 may be associated with tumor characteristics and may affect anti-PD-L1/PD-1 therapy.

Nephrectomy plus systemic chemotherapy is the routine treatment for WT. For most patients, standard therapy can achieve satisfactory results. But for patients with recurrence or more aggressive disease, combination chemotherapy is usually administered.[27,28] For WT patients with poor prognosis, considering the side effects of chemotherapy, immune checkpoint inhibitors may be a feasible selection. The study of plasma ePD-L1 in WT patients is helpful for the choice of immunotherapy.

In summary, our results demonstrated that the significantly increased plasma ePD-L1 levels in WT patients were biologically active in suppressing the activation of CD8^{+} T cells, and were significantly correlated with intracellular TNFα production in peripheral CD8^{+} T cells of WT patients. Further studies are needed to validate their potential role in WT patients.

Ethical Approval

Declaration of Conflicting Interests

Funding

ORCID iD

Guoliang Wang https://orcid.org/0000-0002-9191-6166

References

1. Oh L, Hafsi H, Hainaut P, Ariffin H. P53, stem cell biology and childhood blastomas. *Curr Opin Oncol*. 2019;31(2):84-91.

2. Leslie SW, Sajjad H, Murphy PB. Wilms tumor. In: *StatPearls [Internet]*. Treasure Island (FL): StatPearls Publishing; 2021.

3. Rossoff J, Tse WT, Duerst RE, et al. High-dose chemotherapy and autologous hematopoietic stem-cell rescue for treatment of relapsed and refractory Wilms tumor: re-evaluating outcomes. *Pediatr Hematol Oncol*. 2018;35(5–6):316–321.

4. Zhang W, Lu X, Cui P, et al. Phase I/II clinical trial of a Wilms' tumor 1-targeted dendritic cell vaccination-based immunotherapy in patients with advanced cancer. *Cancer Immunol Immunother*. 2019;68(1):121-130.

5. Chen L, Han X. Anti-PD-1/PD-L1 therapy of human cancer: past, present, and future. *J Clin Invest*. 2015;125(9):3384-3391.

6. Topalian SL, Taube JM, Anders RA, Pardoll DM. Mechanism-driven biomarkers to guide immune checkpoint blockade in cancer therapy. *Nat Rev Cancer*. 2016;16(15):275-287.

7. Ribas A, Hamid O, Daud A, et al. Association of pembrolizumab with tumor response and survival among patients with advanced melanoma. *J Am Med Assoc*. 2016;315(15):1600-1609.

8. Wang X, Teng F, Kong L, Yu J. PD-L1 expression in human cancers and its association with clinical outcomes. *Onco Targets Ther*. 2016;9:5023-5039.

9. Hui E, Cheung J, Zhu J, et al. T cell costimulatory receptor CD28 is a primary target for PD-1-mediated inhibition. *Science*. 2017;355(6332):1428-1433.

10. Yokosuka T, Takamatsu M, Kobayashi-Imanishi W, Hashimoto-Tane A, Azuma M, Saito T. Programmed cell death 1 forms negative costimulatory microclusters that directly inhibit T cell receptor signaling by recruiting phosphatase SHP2. *J Exp Med*. 2012;209(6):1201-1217.

11. Topalian SL, Drake CG, Pardoll DM. Immune checkpoint blockade: a common denominator approach to cancer therapy. *Cancer Cell*. 2015;27(4):450-461.

12. Brahmer JR, Drake CG, Wollner I, et al. Phase I study of single-agent anti-programmed death-1 (MDX-1106) in refractory solid tumors: safety, clinical activity, pharmacodynamics, and immunologic correlates. *J Clin Oncol*. 2010;28(19):3167-3175.

13. Chen G, Huang AC, Zhang W, et al. Exosomal PD-L1 contributes to immunosuppression and is associated with anti-PD-1 response. *Nature*. 2018;560(7718):382-386.

14. Ricklefs FL, Alayo Q, Krenzlin H, et al. Immune evasion mediated by PD-L1 on glioblastoma-derived extracellular vesicles. *Sci Adv*. 2018;4(3):eaar2766.

15. Theodoraki MN, Yerneni SS, Hoffmann TK, Gooding WE, Whiteside TL. Clinical significance of PD-L1+ exosomes in plasma of head and neck cancer patients. *Clin Cancer Res*. 2018;24(4):896-905.

16. Yang Y, Li CW, Chan LC, et al. Exosomal PD-L1 harbors active defense function to suppress T cell killing of breast cancer cells and promote tumor growth. *Cell Res*. 2018;28(8):862-864.

17. Becker A, Thakur BK, Weiss JM, Kim HS, Peinado H, Lyden D. Extracellular vesicles in cancer: cell-to-cell mediators of metastasis. *Cancer Cell*. 2016;30(6):836-848.

18. Ludwig S, Floros T, Theodoraki MN, et al. Suppression of lymphocyte functions by plasma exosomes correlates with disease activity in patients with head and neck cancer. *Clin Cancer Res*. 2017;23(16):4843-4854.

19. Whiteside TL. Exosomes and tumor-mediated immune suppression. *J Clin Invest*. 2016;126(4):1216-1223.

20. Page DB, Postow MA, Callahan MK, Allison JP, Wolchok JD. Immune modulation in cancer with antibodies. *Annu Rev Med*. 2014;65:185-202.

21. Vanella V, Festino L, Strudel M, Simeone E, Grimaldi AM, Ascierto PA. PD-L1 inhibitors in the pipeline: promise and progress. *Oncoimmunology*. 2017;7(1):e1365209.

22. Borcoman E, Nandikolla A, Long G, Goel S, Le Tourneau C. Patterns of response and progression to immunotherapy. *Am Soc Clin Oncol Educ Book*. 2018;38:169-178.

23. Wang G, He L, Wang S, et al. EV PD-L1 is correlated with clinical features and contributes to T cell suppression in pediatric thyroid cancer. *J Clin Endocrinol Metab*. 2020;105(8):e2970-e2981.

24. Wu X, Wang G, Chen X, et al. Impaired T cell-dependent humoral immune response associated with juvenile-onset recurrent respiratory Papillomatosis progression. *Sci Rep*. 2016;6:36378.

25. Cone EB, Dalton SS, Van Noord M, Tracy ET, Rice HE, Routh JC. Biomarkers for Wilms tumor: a systematic review. *J Urol*. 2016;196(5):1530-1535.

26. Poggio M, Hu T, Pai CC, et al. Suppression of exosomal PD-L1 induces systemic anti-tumor immunity and memory. *Cell*. 2019;177(2):414-427.

27. Oostveen RM, Pritchard-Jones K. Pharmacotherapeutic management of Wilms tumor: an update. *Paediatr Drugs*. 2019;21(1):1-13.

28. Saha H, Ghosh D, Biswas SK, Mishra PK, Saha K, Chatterjee U. Synchronous bilateral Wilms tumor: five-year single-center experience with assessment of quality of life. *J Indian Assoc Pediatr Surg*. 2019;24(1):52-60.